# Preparation and Characterization of Aluminium Doped Titanium Dioxide Nanoparticles by Sol-Gel Method for Solar Cell Applications

**K.M.Prabu[1] P.M.Anbarasan[1]**
[1,2]Department of Physics
[1,2]Centre for Nanoscience and Nanotechnology, Periyar University, Salem, Tamil Nadu, India.

*Abstract*— Metal oxide semiconductor nanoparticles play an outstanding role in many applications that are regarded as particularly promising within the broad area of nanotechnology, energy storage, energy conversion and biomedical applications. Among the various semiconductor nanoparticles $TiO_2$ based nanomaterials are various photovoltaic applications. In this present work, we have synthesized Al doped $TiO_2$ nanoparticles by using a sol-gel technique. The prepared samples were investigated optical absorption, functional group, surface morphology and elementary composition of pure $TiO_2$ and Al doped $TiO_2$ nanoparticles by using UV-Visible spectroscopy, FT-IR, Photoluminescence (PL) -studies, FE-SEM and EDS analysis.

***Key words:*** Al doped $TiO_2$ nanopowders and sol-gel method

## I. INTRODUCTION

The nanoparticle is defined as a small object that behave whole unit in terms of transfer to their properties. Nanoparticle is measure metal particles between 10nm and 100nm is used for contains in art, recent technical advances. Nanotechnology is study manipulating matter on atomic and molecular scale; generally nanotechnology is deals with development material device. Nanotechnologies are the design, charactoration production and applications of strictures and controlling by shape and size. The nanotechnology is very diverge range from extension of conversional device physics to completely new approaches based upon molecular self assembly [1-5]. Nano science is the study of phenomena and manipulations of materials at atomic, molecular and macromolecular scale were properties differ significantly from those at large scale. Nonmaterial is regularly proposed should exclude nonmaterials create a form of natural food substance which with is government agree. The shells represent a natural demonstration that a structure conform from nanoparticle is strong. Typical carbon-carbon bond lengths are in the range 0.12-0.5nm and a DNA double helix has a diameter around 2nm. The smallest cellular life forms, the bacteria of the genus mycroplasma are 200nm in length. Nano particle are used as quantum electronics, photonics crystal, DNA clips, bio sensors etc. Nanocrystalline $TiO_2$ has shown excellent performance by comparison to other semiconductors such as ZnO, $SnO_2$, Al, Ag, Mg, Mn, Bi and $Nb_2O_5$. Until now, most of the doping for $TiO_2$ nanomaterials has been explored for photocatalysis [6-10]. The doping effects, however, do not seem so pronounced by comparison to the corresponding undoped $TiO_2$. The energy conversion efficiency remained either unchanged or a little improvement. Over the past decade, nanomaterials have been the subject of enormous interest. Here, we synthesized nanocrystalline metal oxides through the sol-gel process [11-14]. The sol-gel process has become a widely used method during the last several decades. $TiO_2$ nanomaterials are one of the potential candidates for solar energy application due to $TiO_2$'s unique optoelectronic and photochemical properties. Especially, as a photovoltaic performance to efficient energy conversion for solar irradiations, $TiO_2$ nanomaterials have been receiving a great deal of attention. $TiO_2$, especially its anatase phase, has attracted much attention for its potential application in degradation of various environmental pollutants, both gaseous and liquid. However; its short comings include a large band gap (~3.2 eV) which causes most of the solar spectrum unutilized. To extend the optical absorption of $TiO_2$ to the visible region, various dopants have been added to the oxide to improve its solar efficiency [15-20].

## II. MATERIALS AND METHODS

### A. Chemicals Used

Most of the Chemicals used in the research are standard chemicals that are normally available in the laboratory. The chemicals used in this study were titanium isopropoxide, Aluminum nitrate; glacial acetic acid absolute ethanol and methanol were bought from Sigma-Aldrich. All the chemicals were used without further purification.

### B. Sample preparation

Metal oxide nanoparticles attract great attention in recent years on account of their special electronic and chemical properties. In this paper, Al doped $TiO_2$ nanoparticles with high photo catalytic activity were synthesized by sol-gel method. The nano $TiO_2$ powder was prepared with titanium isopropoxide solution as the raw material. In a typical experiment, 0.05 mol % Aluminium nitrate were dissolved in 60 ml of deionized water at room temperature, followed by adding 5 ml of glacial acetic acid to obtain solution A. 14 ml titanium isopropoxide was dissolved in 40 ml of anhydrous ethanol with constant stirring to form solution B. Then, the solution B was added drop-wise into the solution A within 2 hours under constant stirring. Subsequently, the obtained sol was stirred continuously for 3 h and aged for 3 days at room temperature. As-prepared TiO2 gels were dried for 10h at 80°C. The obtained solids were ground and finally calcinated at 500°C for 2 h (heating rate = 5°C/min).

## III. RESULTS AND DISCUSSION

### A. UV-Visible Absorption Spectroscopy

Absorption spectroscopies are powerful non- destructive techniques to explore the optical properties of semiconducting nanoparticles. The UV–Visible spectrum of modified $TiO_2$ nanopowders was obtained to determine the relationship between the solar energy conversion efficiency and spectroscopic property. The UV-Visible spectral studies of the pure $TiO_2$, Al doped $TiO_2$ were carried out using Lambda 35 model UV-visible spectrometer in the range of

 

200 to 1100 nm. The photo absorption of Al doped $TiO_2$ in the visible-light region was stronger than that of pure $TiO_2$. The modified $TiO_2$ nanopowders were calcined at 500ºC the visible-light photo absorption is strongest and it produces high photocatalyactivity. The energy gap ($E_g$) is determined by the equation (1),

$$E_g = 1242/\lambda \qquad (1)$$

Where λ (nm) is the wavelength of the absorption edge in the spectrum. \

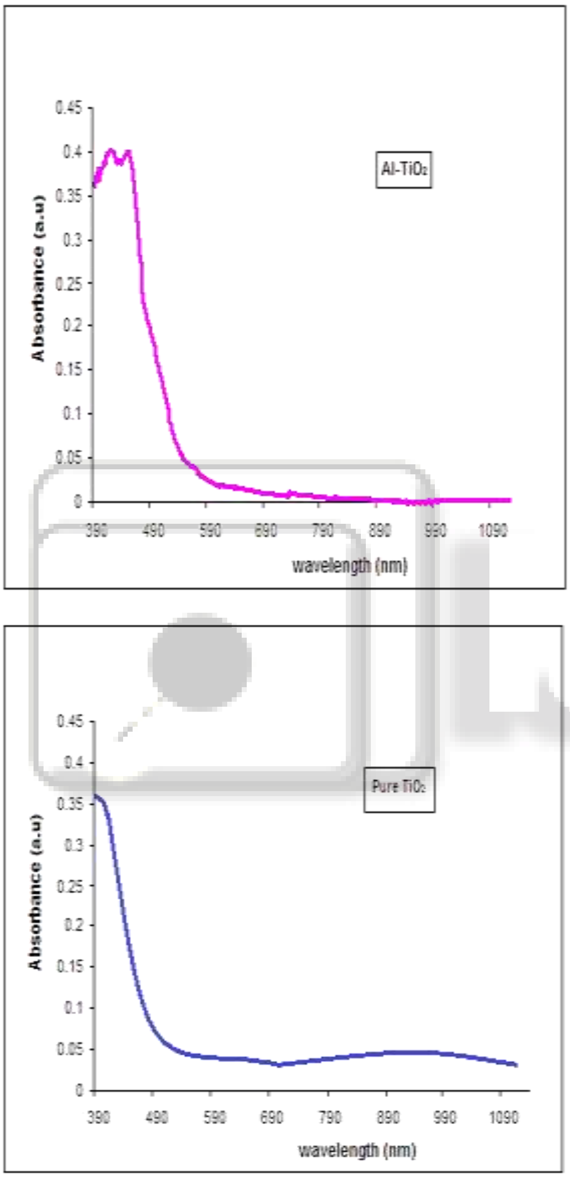


Fig. 1: UV-visible spectra of (a) Pure $TiO_2$ (b) Al-$TiO_2$

The cut-off wavelength of pure and Al doped $TiO_2$ is 410 nm & 490 nm and its corresponding its band gap value is 3.029 & 2.5346. These results concluded that the Al doped $TiO_2$ nanopowders to the small band gap compare to other pure $TiO_2$. The absorption spectrum of Al doped $TiO_2$ shows that the small band gap in the entire visible region and it is a good candidate for solar cell applications. The energy gaps of modified $TiO_2$ shows mostly visible region and exhibits broad absorption compare to pure $TiO_2$

### B. *Fourier Transform Infrared Analysis (Ft-Ir).*

The Fourier transform infrared (FTIR) Spectra of pure and Al doped $TiO_2$ nanopowders were recorded in the range of 4000 – 400 $cm^{-1}$ using KBr pellet technique Perkin Elmer spectrometer. The recorded FTIR spectrum of pure $TiO_2$ & Al doped $TiO_2$ are shown in figure 2.

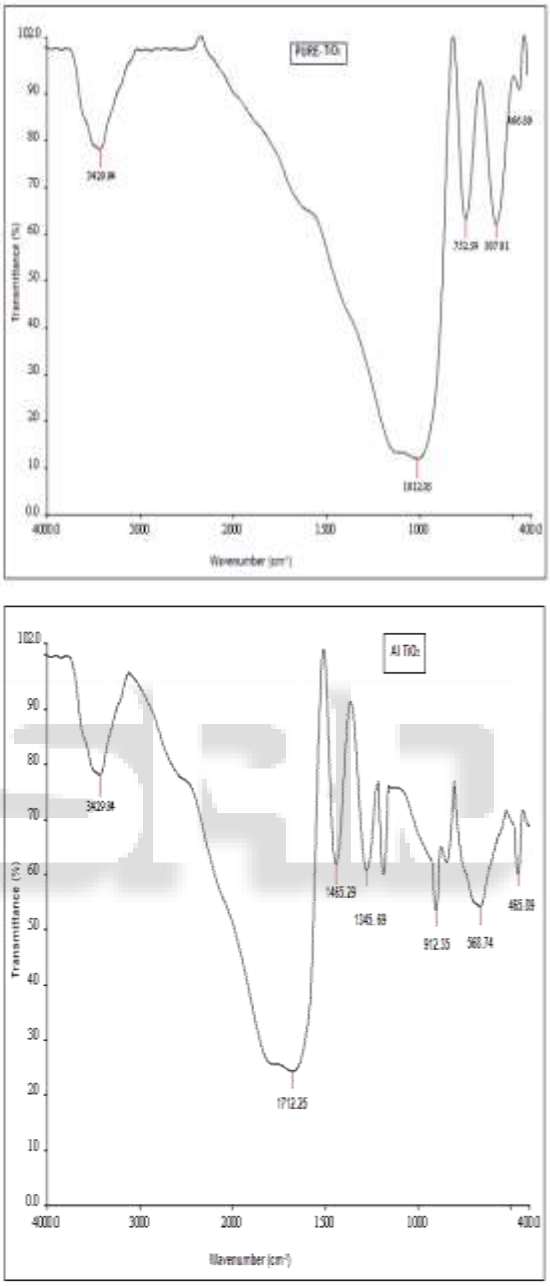


The different bonds and functional groups absorbed at different wavelengths, an infrared spectrum is used to determine the structure of organic molecules. Although this radiation is weak, it does supply sufficient energy for bonds in the molecule to vibrate by Stretching or Bending. The area from 3500 $cm^{-1}$ to 1300 $cm^{-1}$ is called the functional group region. The bands in this region are particularly useful in determining the type of functional groups present in the molecule. The area from 1300 $cm^{-1}$ to 667 $cm^{-1}$ is called the fingerprint region. A peak-by-peak match of an unknown spectrum with the spectrum of the suspected compound in this region can be used, much like a fingerprint, to conform its identity. The reaction between precursor materials of both pure and various oxide doped $TiO_2$ nanopowders are prepared by sol-gel method. The absorption band was observed in the range 3429-3429 $cm^{-1}$ for pure and aluminium doped $TiO_2$ nanoparticles, which was described to the both symmetric and asymmetric stretching vibrations of the hydroxyl group. Whereas, the characteristic peaks between 1712 $cm^{-1}$ is associated with the O-H banding vibration of the absorbed water molecules. The C-H bending is observed at 1012, 1465 & 1345 $cm^{-1}$ in the compound type of alcohols present in both samples. In the spectrum of pure $TiO_2$, the peak at 466 $cm^{-1}$ should be attributed to Ti-O bond in the $TiO_2$ lattice (anatase titanium). For aluminium doped $TiO_2$ nanoparticles & pure $TiO_2$ nanoparticles, the peaks locked in the region 568 & 587 $cm^{-1}$ indicating the Ti-O-O band. The bands between 750-650 $cm^{-1}$ illustrate the Ti-O-Ti stretching vibration. Figure 2 FT-IR spectra of Pure $TiO_2$ & Al-$TiO_2$

*C. Photo Luminescent (PL) studies*

Photoluminescence emission spectra of Pure $TiO_2$ & Al doped $TiO_2$ are shown in Fig.3 (a) & (b) respectively. The PL emission spectra exhibits emission peaks range of 300 nm -700 nm. In the PL characteristics of pure $TiO_2$ nanoparticles to display a blue photoluminescence band width strong intensity and sharp features centered at approximately 350 nm. The PL characteristics of Al doped $TiO_2$ nanoparticles to display a strong intensity band width and broad features centered at approximately 420 nm, 400 nm - 500 nm region. It exhibits a green luminescence and it is frequently attributed to bulk defects, such as dislocations and stacking faults, and deep-level traps. The bulk defects were not found in modified $TiO_2$ nanoparticles. The green-shifted emission was then ascribed to the band gap reduction of $TiO_2$ due to its high density of states close to the conduction band minimum and the subsequent filling of conduction band edge by additional depended material induced carriers. The green band emission in the present study may be due to the acceptor levels related to interstitial aluminium and donor levels due to native defects mostly occur in Al doped $TiO_2$ phase.

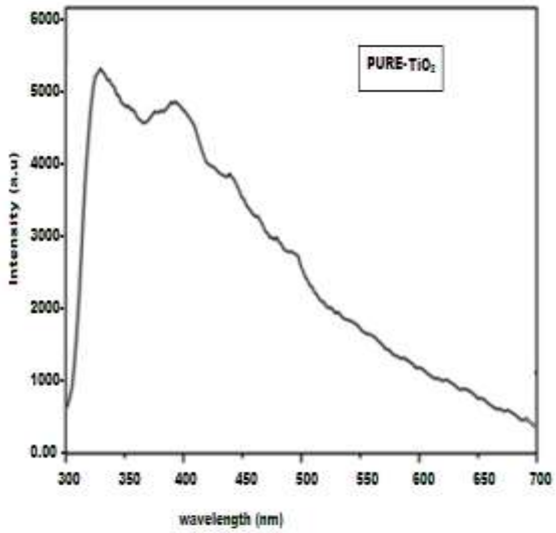


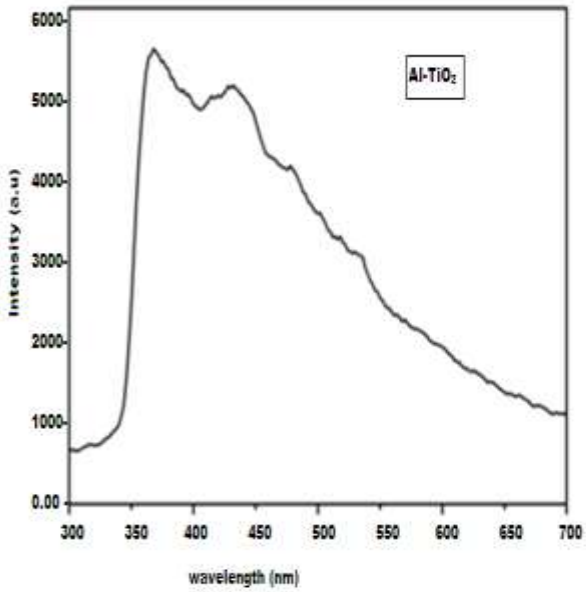


Fig. 3: PL-studies of Pure $TiO_2$ & Al-$TiO_2$

*D. Field Emission Scanning Electron Microscopy (FE-SEM) Analysis*

Figure 4 (a & b) shows the FESEM micrographs of the pure and Al doped $TiO_2$ nanoparticles prepared by sol-gel method. The FE-SEM micrographs of the pure $TiO_2$ nanoparticles depicted has non-uniform distribution of spherical particles.

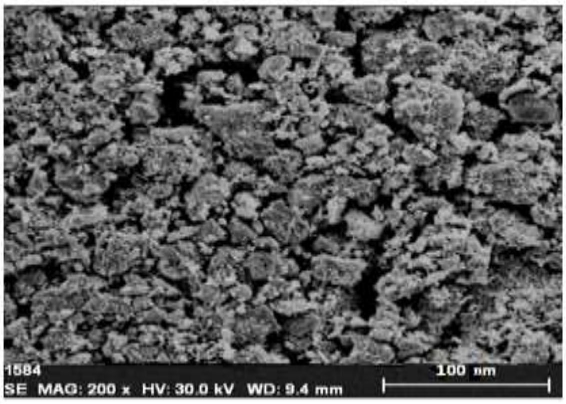


Fig. 4(a)

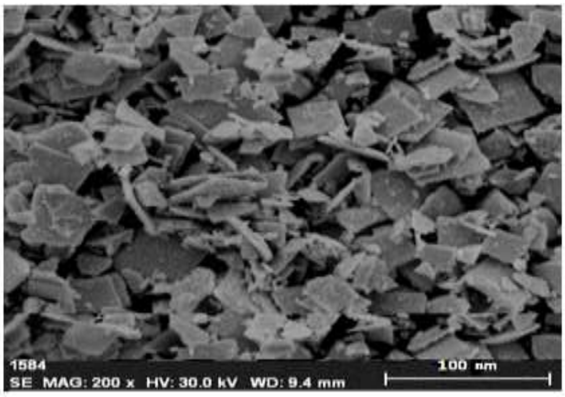


Fig. 4(b)

Fig. 4: FESEM Micrographs 4 (a) Pure $TiO_2$ (b) Al-$TiO_2$

The FE-SEM analysis reveals that the morphology of Al doped $TiO_2$ was smooth and well defined rectangular shape with grain size 30-60 nm with minimal agglomeration compare to pure $TiO_2$. It has been observed that the $TiO_2$ nanoparticles annealed at 500ºC were almost reveals that the primary particles are quite uniform in size, quite clean and roughly spherical in shape, and that the agglomerates are fused together to form comparatively smaller irregular grains giving rise to highly porous materials which enhancing the photovoltaic performance.

*E. EDS Analysis*

The semi quantification of elemental analyses to identify the weight percentage of major and minor elements present in the samples were done using Energy Dispersive X-ray Spectrometer (EDS),JEOL model, JSD-5610 LV with an accelerating voltage of 20KV. The result of energy dispersive X-ray spectroscopic (EDS) analysis of pure $TiO_2$ and Al doped $TiO_2$ nanopowders are shown in fig 5(a) & 5 (b).

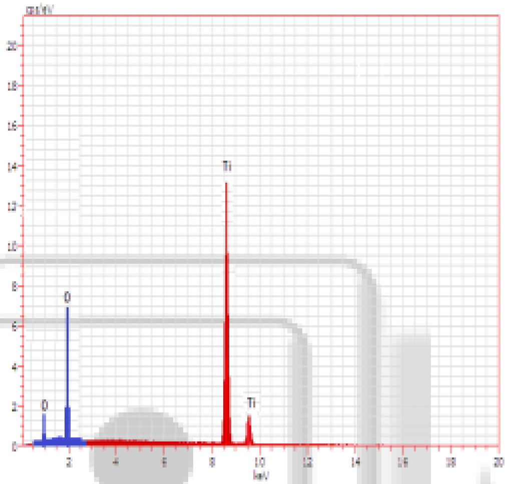


Fig. 5 (a)

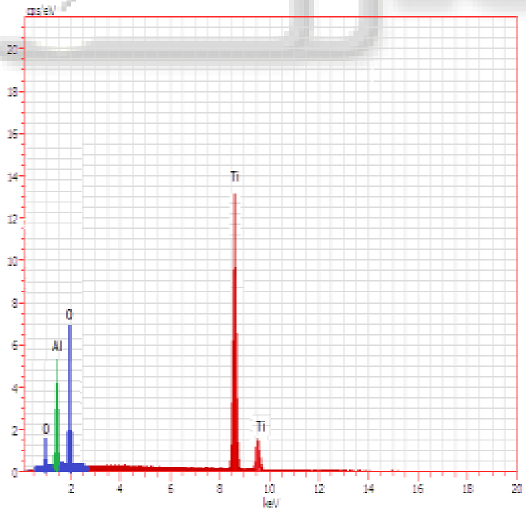


Fig. 5: (b) Figure 5 EDS Analysis (a) Pure $TiO_2$ (b) Al-$TiO_2$

Trace elements are estimated by determining the percentage abundance of elements such as Ti, O & Al present in the sample. The concentration of titanium, oxygen and aluminum is shown in table.

| **Sample** | **Element** | **Weight (%)** | **Atomic (%)** |
|---|---|---|---|
| Pure $TiO_2$ | O K | 30.20 | 58.42 |
| | Ti K | 69.80 | 41.58 |
| | Total | 100.00 | 100.00 |

Table 2 (a)

| **Sample** | **Element** | **Weight (%)** | **Atomic (%)** |
|---|---|---|---|
| Al- $TiO_2$ | O K | 36.24 | 62.10 |
| | Ti K | 61.10 | 35.15 |
| | Ag K | 2.66 | 2.75 |
| | Total | 100.00 | 100.00 |

Table 2 (b)

Table 2: EDS Analysis of (a) Pure $TiO_2$ (b) Al-$TiO_2$

## IV. CONCLUSION

The pure and Al doped $TiO_2$ nanoparticles were successfully prepared by sol-gel method. The UV-Visible and PL result shows Al doped titanium nanoparticles extend the absorption edge ultraviolet to visible range and make the green shift more distinct and also analyses the band gap value. The Ti-O bond of anatase phase in all the synthesized samples was identified by FT-IR measurements. The FE-SEM analysis reveals that the morphology of Al doped $TiO_2$ was smooth and well defined rectangular shape with grain size 30-60 nm with minimal agglomeration compare to pure $TiO_2$. Also analyses the morphology of doped $TiO_2$ was regular arrangement, spherical shape, uniform size, and good packing density. The doped and pure elements are identified from EDX spectrum, in which the spectrum confirms the aluminium is presented in doped samples.

## REFERENCES

[1] Rong-Ho Lee, Yu-Wei Huang, Thin Solid Films, 517, 5903-5908, (2009).
[2] O. Carp, C. L. Huisman, A. Reller, Progress in Solid State Chem., 32, 33, (2004
[3] C. S. Kim, K. Okuyama, K. Nakaso, M.Shimada, Direct measurement of nucleation and growth modes in titania nanoparticles generation by a CVD method, J Chem Eng Jpn, 37(11), 1379, (2004).
[4] K. Nazeeruddin, R. Humphry-Baker, P. Liska, M. Gratzel, J. Phys. Chem., B 107, 8981, (2003).
[5] S. Uchida, R. Chiba, M. Tomiha, N. Masaki, M. Shirai, Electrochemistry 70, 418, (2002).
[6] M. Adachi, Y. Murata, J. Takao, J. Liu, M. Sakamoto, F. Wang, J. Am. Chem. Soc. 126 ,14943, (2004).
[7] J. Jiu, S. Isoda, F. Wang, M. Adachi, J. Phys. Chem., B 110, 2087.
[8] C. Flores, J.N. de Freitas, C. Longo, M.A. De Paoli, H. Winnischofer, A.F. Nogueira, J. Photochem. Photobiol. A Chem. 189, 153, (2007).
[9] S. Chappel, S.G. Chen, A. Zaban, Langmuir 18, 3336, (2002).
[10] Bedja, P.V. Kamat, X. Hua, A.G. Lappin, S. Hotchandani, Langmuir 13 ,2398, (1997).
[11] K. Keis, C. Bauer, G. Boschloo, A. Hagfeldt, K. Westermark, H. Rensmo, H. Siegbahn, J. Photochem. Photobiol. Chem. 148, 57, (2002).
[12] S. Chappel, A. Zaban, Solar Energy Mater Solar Cells, 71,141, (2002).

[13] P. Guo, M.A. Aegerter, Thin Solid Films, 351, 290, (1999).
[14] C. Jones, P. R. Chalker, J. Phys. D: Appl. Phys., 36, 80, (2003).
[15] K. L. Choy, Prog. Mater. Sci., 48, 164, (2003).
[16] R. Van de Krol, A. Goossens, J. Schoonman, J. Electrochem. Soc., 144, (1997).
[17] M. Gratzel, J. Photochem. Photobiol. C 4, 145, (2003).
[18] Kyung Hyun Ko, Young Cheol Lee, Young Jin Jung, Journal of Colloid and Interface Science, 283, 482-487, (2005).
[19] A. C. Pierre, Introduction to sol-gel processing, Kluwer Academic Publishers: Boston, 394 (1998).
[20] Jin Young Kim & Sangwook Lee & Jun Hong Noh & Hyun Suk Jung & Kug Sun Hong, J. Electroceram. 23 ,422-425, (2009).